Theory of continuously distributed trap states at Si-SiO_2 interfaces

T. Sakurai and T. Sugano
Department of Electronic Engineering, The University of Tokyo, Bunkyo-ku, Tokyo 113, Japan

(Received 7 August 1980; accepted for publication 1 December 1980)

A calculation method to treat the electronic structures of crystalline Si-amorphous SiO_2 interfaces with or without microstructural defects is developed based on semiempirical tight-binding Hamiltonians and the Green's function formulation, and applied for calculation of the energy level of the trap states between amorphous SiO_2 and the Si substrate with (111) orientation. The major results are (i) the perfect interface does not have any states in the forbidden gap of Si although the Si-O-Si bonding angle at the interface is varied in the range between 120° and 180°, and neither does the interface with oxygen dangling bonds have any; (ii) trap states due to a Si dangling bond appear at about the middle of the Si band gap; and (iii) O-vacancy and Si-Si weak bonds at the interface produce trap states at the energy range higher than the midgap, whereas Si-O weak bonds at the interface produce trap states at the energy range lower than the midgap. The energy level of these trap states varies with changing bonding parameters such as bond lengths and bond angles. These energy levels caused by Si-Si weak bonds and Si-O weak bonds are possible origins of the interface states continuously distributed in energy. The reduction of trap states in the Si forbidden gap by bonding H, OH, Cl, and F atoms to Si dangling bonds is also discussed.

PACS numbers: 73.20.Hb, 73.40.Qv, 71.10. + x, 71.25Rk

I. INTRODUCTION

The trap states between the Si-SiO_2 interface have been attracting much attention because these states take an important role in controlling the threshold voltage V_{th}, transconductance, and flicker noise of metal-oxide-semiconductor (MOS) transistors. However, the chemical and physical origins of these states have not been fully understood, although some attempts were made to shed light on these problems by Chadi *et al.*[1-3] In particular, little is known about the theoretical background of the fact that these interface trap states are continuously distributed in energy. Our work is an extension of the approach of Chadi *et al.* with a special emphasis on this continous distribution of the trap states at Si-SiO_2 interfaces.

Our basic model has been constructed with a crystalline Si with (111) orientation and amorphous SiO_2 represented by a Bethe-lattice as shown in Fig. 1. This can be considered as a Cluster-Bethe-lattice model (CBLM) first introduced by Joannopoulos and Yndurain,[4] but in our case the cluster is the crystalline silicon, whose dangling bonds are terminated by the SiO_2 Bethe-lattices. The experimental evidences for a very thin Si-SiO_2 transition layer[5,6] and the theoretical conclusion that the elastic energy of the Si-SiO_2 system is lowered as the width of the SiO_x layer goes toward zero,[7] encourage us to use this idealized abrupt-junction model to simulate a thermally grown SiO_2-Si interface. Since oxygen chemisorption of a 1/3 monolayer on a Si free surface is enough to cancel the surface reconstruction,[8] it is not needed to include the reconstruction of crystalline Si surface at the interface.

A Bethe-lattice used here to represent amorphous SiO_2 is a hypothetical, tree-like lattice containing no closed rings, where the valencies of O and Si are maintained two and four, respectively. It is constructed by connecting SiO_4 tetrahedrals and has threefold symmetry. A normal Si-O-Si angle is chosen to be 144°, which is believe to be the peak value of a Si-O-Si angle in an amorphous SiO_2 system,[9] and this angle is varied in the range between 120° and 180° in case of an amorphous effect. The electronic structures of crystalline SiO_2 and amorphous SiO_2 are shown to be similar by optical absorption measurements,[10] though the long-range atomic configurations are quite different. This suggests that the short-range orders such as valencies and SiO_4 tetrahedrals play an important role to determine the electronic structures, so that the Bethe-lattice model is thought to be a good approximation to represent amorphous SiO_2.

Based on this basic model we have calculated the energy levels of microscopic defects at Si-SiO_2 interfaces with changing various bonding parameters such as bond lengths, bond bending angles, and bond rotation angles and investigated the possible origins of the interface traps continuously distributed in the forbidden gap of Si. Furthermore, we have

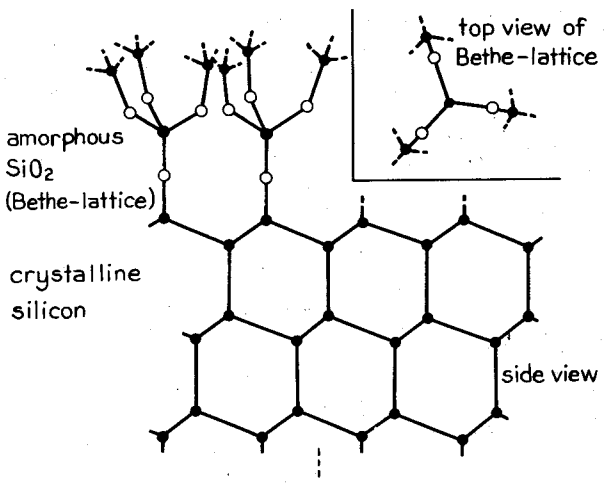

FIG. 1. Basic model constructed with amorphous SiO_2 represented by Bethe-lattice and Si substrate with (111) orientation. Open and closed circles denote O and Si atoms, respectively.

 0021-8979/81/042889-08$01.10

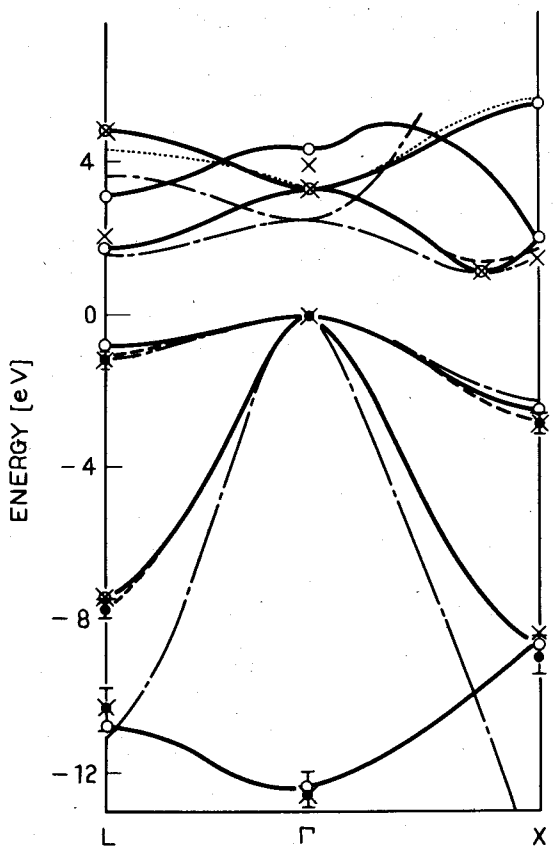

FIG. 2. Calculated energy-band structure of bulk silicon using tight-binding Hamiltonians. Solid line denotes calculated result by the authors, broken line by Pandey and Phillips (Ref. 11), dot-dashed line by Dresselhaus and Dresselhaus (Ref. 12), dotted line by Chadi (Ref. 13), X by pseudopotential method (Ref. 14), and closed circle with error bar denotes experimental observation (cf. Ref. 11). In the present work Si band gap is calculated to be 1.1 eV, which agrees with the experimental result. The top of valence band is chosen energy zero.

obtained the energy levels of impurities such as H, OH, Cl, and F bonded to Si dangling bonds at the interface and discussed the annealing behavior of the interface traps.

Section II of this paper is devoted to the formulation of Hamiltonians, Sec. III deals with the calculation method based on Green's function, Sec. IV shows the models of the microstructural defects, and Sec. V describes the results and discussions.

II. HAMILTONIAN FORMULATION

A semiempirical formulation of parametrized Hamiltonians in which various interaction parameters among valence electrons are determined so as to fit the calculated band structure to the experimental results and the band structure calculated by the pseudopotential method was used for SiO_2 and Si. The values of the parameters for SiO_2 were given by Chadi *et al.*[2] For crystalline Si, the agreement of the band structure calculated by using previously published parameters[11–13] with the band structure which was experimentally known[11] and calculated by the pseudopotential method[14] are not necessarily satisfactory, so that the parameters up to second nearest-neighbor interactions have been determined to improve the results with special care to fit the band gap to 1.1 eV because we are interested in this energy range. The band structures for Si by the previously published parametes and newly determined parameters are shown in Fig. 2. The values of parameters are given in Table I in standard notation.[15]

In varying the bond length, we assume that each interaction parameter is altered according to

$$V_{ij}(R_{kl}) = V_{ij}(R^0_{kl})[S_{ij}(R_{kl})/S_{ij}(R^0_{kl})]\,, \tag{1}$$

within the approximation of the extended Hückel theory. In Eq. (1) the interaction parameter $V_{ij}(R_{kl})$, and the overlap integral $S_{ij}(R_{kl})$ are those at the bond length R_{kl}, and R^0_{kl} denotes the bulk bond length.

When impurities (H or Cl or F) are associated, a method based on the extended Hückel theory[16] has been used. The ij element of the Hamiltonian is calculated as

$$H_{ij} = -KS_{ij}(\mathrm{VOIP}_i + \mathrm{VOIP}_j)/2, \tag{2}$$

$$H_{ii} = \mathrm{VOIP}_i\,,$$

where S_{ij} is the overlap integral between the ith and jth orbitals, VOIP_i the valence orbital ionization potential of the ith orbital whose value was given by Basch *et al.*,[17] and K the proportionality constant. K has been changed in the range between 1.0 and 2.0 since this range is empirically believed to be probable,[16,18] but the conclusion described in Sec. V has not been affected by the choice of K value. In calculating S_{ij}, the atomic orbitals were approximated by Slater-type orbitals with Clementi's orbital exponents.[19] The nearest-neighbor interactions among valence orbitals were taken into account.

III. GREEN'S FUNCTION FORMULATION

Once the Hamiltonian has been established, the next problem is how to obtain the eigenvalues because the size of the Hamiltonian is extremely large and therefore straightforward solving is impossible. A Green's function formulation is convenient for this purpose. The Green's function G is defined as

$$G(E) = (EI - H)^{-1} = \sum_n \frac{|E_n\rangle\langle E_n|}{E - E_n}\,, \tag{3}$$

where E denotes energy, I a unit matrix, H a Hamiltonian, and E_n and $|E_n\rangle$ the nth eigenvalue and eigenvector, respectively. The local density of states of the jth orbital (LDOS_j) is

TABLE I. Interaction parameters (in eV). The superscripts 1 and 2 refer to first and second nearest-neighbor interactions, respectively.

E_s	E_p	V^1_{ss}	V^1_{sp}	$V^1_{pp\sigma}$	$V^1_{pp\pi}$	V^2_{ss}	V^2_{sp}	$V^2_{pp\sigma}$	$V^2_{pp\pi}$
−10.44	−4.101	−2.144	2.090	2.346	−0.588	0.123	−0.366	0.435	−0.154

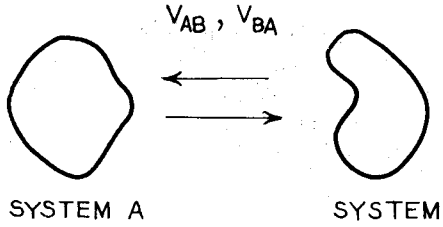

FIG. 3. Schematic illustration that systems A and B interact with each other.

expressed as

$$\mathrm{LDOS}_j = \sum_n |\langle j|E_n\rangle|^2\,\delta(E-E_n)$$

$$= -(1/\pi)\lim_{\delta\to+0} I_m\,[G(E+i\delta)_{jj}]\,, \tag{4}$$

where $I_m\,[G(E+i\delta)_{jj}]$ is an imaginary part of the jj element of the matrix $G(E+i\delta)$.

Here it must be notified that the matrix size to be manipulated is greatly reduced if the interactions among atoms are short ranged. When systems A and B interact with each other through short-range interaction as shown in Fig. 3, the Hamiltonian and Green's function G, respectively, are written in the form

$$(EI-H)^{-1} = \left[EI - \begin{pmatrix} h^{22}_{AA} & h^{21}_{AA} & 0 & 0 \\ h^{12}_{AA} & h^{11}_{AA} & V^{11}_{AB} & 0 \\ 0 & V^{11}_{BA} & h^{11}_{BB} & h^{12}_{BB} \\ 0 & 0 & h^{21}_{BB} & h^{22}_{BB} \end{pmatrix}\right]^{-1}, \tag{5}$$

$$G(E) = \begin{pmatrix} G^{22}_{AA} & G^{21}_{AA} & G^{21}_{AB} & G^{22}_{AB} \\ G^{12}_{AA} & G^{11}_{AA} & G^{11}_{AB} & G^{12}_{AB} \\ G^{12}_{BA} & G^{11}_{BA} & G^{11}_{BB} & G^{12}_{BB} \\ G^{22}_{BA} & G^{21}_{BA} & G^{21}_{BB} & G^{22}_{BB} \end{pmatrix}. \tag{6}$$

On the other hand, when the systems A and B are independent, as illustrated in Fig. 4, the Green's function for each system g_{AA} and g_{BB} are written as

$$g_{AA} = \left[EI - \begin{pmatrix} h^{11}_{AA} & h^{12}_{AA} \\ h^{21}_{AA} & h^{22}_{AA} \end{pmatrix}\right]^{-1} = \begin{pmatrix} g^{11}_{AA} & g^{12}_{AA} \\ g^{21}_{AA} & g^{22}_{AA} \end{pmatrix}, \tag{7}$$

and

$$g_{BB} = \left[EI - \begin{pmatrix} h^{22}_{BB} & h^{21}_{BB} \\ h^{12}_{BB} & h^{11}_{BB} \end{pmatrix}\right]^{-1} = \begin{pmatrix} g^{22}_{BB} & g^{21}_{BB} \\ g^{12}_{BB} & g^{11}_{BB} \end{pmatrix}, \tag{8}$$

respectively.

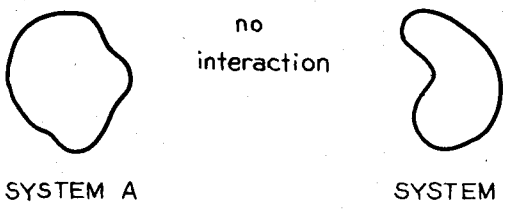

FIG. 4. Schematic illustration that systems A and B are independent.

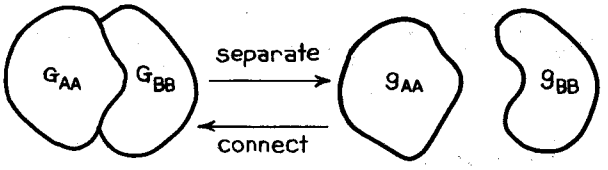

FIG. 5. Schematic illustration of connecting and separating two systems.

Then the following equations are obtained (Appendix A).

$$G^{11}_{AA} = [(g^{11}_{AA})^{-1} - V^{11}_{AB}\,g^{11}_{BB}\,V^{11}_{BA}]^{-1} \tag{9}$$

(equations for connection),

$$g^{11}_{AA} = [(G^{11}_{AA})^{-1} + V^{11}_{AB}\,g^{11}_{BB}V^{11}_{BA}]^{-1} \tag{10}$$

(equation for separation).

These two equations show that the size of the matrix is small if the local density of states within a small part of the system is to be calculated. Moreover, connection and separation of atomic groups as illustrated in Fig. 5 can be done quite easily using these two equations. For example, if system A is the crystalline Si and system B is the amorphous SiO_2, then using Eq. (9), the Green's functions near the interface are calculated, and if G_{AA} is a Green's function of the cyrstalline Si at the perfect interface and g_{BB} is a Green's function of a Bethe-lattice and an extra oxygen atom, then using Eq. (10), the Green's function of the interface including a dangling bond (g_{AA}) can be obtained.

Here, the application of this method to the Si (111) surface is described. Let $\mathbf{k}$ be a two-dimensional reciprocal vector of the Si (111) surface. Then, taking Bloch orbitals as a basis set, the Hamiltonian $H^{\mathbf{k}}$ and the Green's function $G^{\mathbf{k}}$ for a certerin $\mathbf{k}$ vector are expressed in the form

$$G^{\mathbf{k}}(E) = (EI - H^{\mathbf{k}})^{-1}$$

$$= \left[EI - \begin{pmatrix} h^{\mathbf{k}}_{11} & V^{\mathbf{k}}_{1s} & & & \\ V^{\mathbf{k}}_{s1} & h^{\mathbf{k}}_{11} & & 0 & \\ & & V^{\mathbf{k}}_{1s} & & \\ & V^{\mathbf{k}}_{s1} & h^{\mathbf{k}}_{11} & V^{\mathbf{k}}_{1s} & \\ 0 & & V^{\mathbf{k}}_{s1} & h^{\mathbf{k}}_{11} & \ddots \\ & & & \ddots & \ddots \end{pmatrix}\right]^{-1}$$

$$= \begin{pmatrix} G^{\mathbf{k}}_{11} & \\ & * \end{pmatrix}, \tag{11}$$

where $h^{\mathbf{k}}_{11}$, $V^{\mathbf{k}}_{s1}$, $V^{\mathbf{k}}_{1s}$, and $G^{\mathbf{k}}_{11}$ are 8×8 matrices.

Taking into account the fact that the semi-infinite solid should not be influenced by the addition of one atomic layer on the surface [hereafter we will call this technique the layer stacking method (see Fig. 6)], the self-consistent equation for $G^{\mathbf{k}}_{11}$,

$$G^{\mathbf{k}}_{11} = [(E+i\delta)\,I - h^{\mathbf{k}}_{11} - V^{\mathbf{k}}_{1s}\,G^{\mathbf{k}}_{11}V^{\mathbf{k}}_{s1}]^{-1}\,, \tag{12}$$

holds, which is derived by the use of Eq. (9). $G^{\mathbf{k}}_{11}$ can be determined by this equation. To solve Eq. (12) in terms of

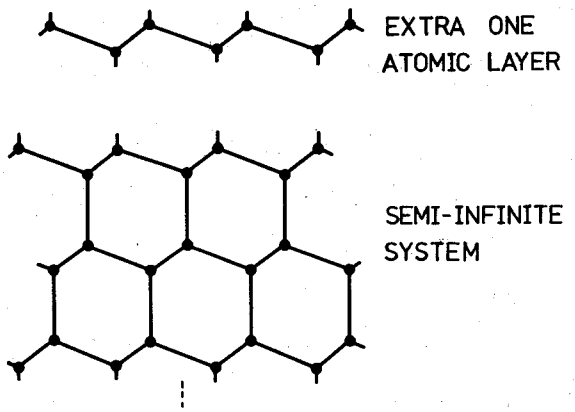

FIG. 6. Layer stacking method. When the system is semi-infinite, it should not be influenced by the addition of the extra one atomic layer.

$G^{\mathbf{k}}_{11}$ numerically, the relaxation method is effective. Since this relaxation process is rather oscillatory, the damping type procedure must be efficient to accelerate the convergence. In fact averaging operation over each oscillation period has shortened the computation time by a factor of 2–10. Once the $G^{\mathbf{k}}_{11}$'s for various $\mathbf{k}$ vectors are obtained, the Green's function G_{11} which takes normal atomic orbitals as a basis set is calculated by

$$G_{11} = \sum_{\mathbf{k}} G^{\mathbf{k}}_{11} \,. \tag{13}$$

The Green's function for the SiO_2 is also calculated by use of an equation of self-consistency. Since the SiO_2 Bethe-lattice employed here has been constructed by infinitely connecting SiO_3 units, one SiO_3 unit whose three oxygen dangling bonds are terminated by the SiO_2 Bethe-lattices is equal to the SiO_2 Bethe-lattice itself. This fact leads to the equation of self-consistency similar to Eq. (12). The Green's function of SiO_2 Bethe-lattice is determined through this equation, where the manipulation of matrices sized 16×16 are required. The solution of the SiO_2 Bethe-lattice is first obtained by Laughlin and Joannopoulos[20] using a transfer matrix technique. In the present method, however, the Green's functions are computed directly without transfer matrices.

When the $i\delta$ in Eq. (4) is approximated by a finite value, owing to the practical limitation, the δ function in Eq. (4) has the Lorentzian broadness. That is, a sharp line spectrum at E_n is broadened by a factor of $\delta/[(E-E_n)^2+\delta^2]$. However, if the values y_1 and y_2 at two points E_1 and E_2 near the peak are given, then the peak value y_p and the peak energy E_p can be calculated by the following formulas,

$$E_p = \{(y_1E_1 - y_2E_2) + [y_1y_2(E_1-E_2)^2 - \delta^2(y_1-y_2)^2]^{1/2}\}/(y_2-y_1)$$
$$y_p = y_1[1+(E_1-E_p)^2/\delta^2] \,. \tag{14}$$

The explanation of y_1, y_2, y_p, E_1, E_2, and E_p is given in Fig. 7. Therefore, though $\delta = 0.04$ eV and energy step of 0.1 eV are adopted here, the error of calculated by this approximation is less than 0.01 eV with help of Eq. (14).

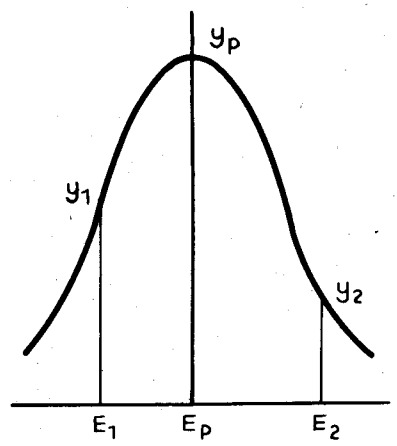

FIG. 7. Lorentzian curve. If E_1, y_1, E_2, and y_2 are known, E_p and y_p can be calculated.

IV. MODELS AND CALCULATION PROCEDURE

Models of the atomic configurations used in the calculation are shown schematically in Fig. 8(a)–18(f). The following is the procedure of the calculation. (1) Fix one certain $\mathbf{k}$ vector. (2) Calculate the Green's function for Si (111) free surface [Fig. 8(a)]. (3) Connect a Bethe-lattice and one oxygen to this surface [Fig. 8(b)]. (4) Sum up the Green's functions over various $\mathbf{k}$ vectors. (5) Separate the Bethe-lattice and one oxygen to form a $Si_3{\equiv}Si$- dangling bond [Fig. 8(c)]. (6) Bring the Bethe-lattice closer to the Si dangling bond to simulate Si-Si bonding and O-vacancy [Fig. 8(d)]. (7) Bring the Bethe-lattice and one oxygen closer to the Si dangling bond to form Si-O weak bond at the interface [Fig. 8(e)]. (8) Bond any of H, O, OH, Cl, or F to the Si dangling bond to represent the bonding of impurity atom [Fig. 8(f)].

These are the rough sketches of the calculation procedure and other atomic configurations used in the calculation will be shown schematically in each time in the results. The normal bond lengths between O and H, Si and O, Si and H, Si and Cl, and Si and F are chosen to be 0.97, 1.61, 1.50, 1.50, and 1.50 Å, respectively.

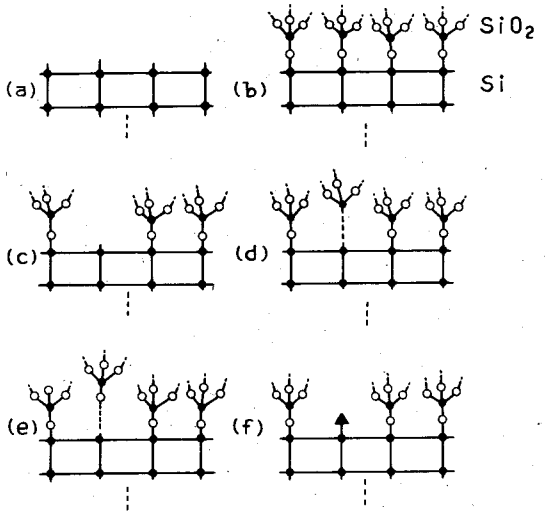

FIG. 8. Models of various configurations used in the calculation. (a) Si free surface, (b) perfect interface, (c) $Si_3{\equiv}Si$- dangling bond, (d) Si-Si weak bond and O-vacancy at interface, (e) Si-O weak bond at interface, (f) impurity at interface. Closed circle, open circle, and closed triangle denote Si, O, and impurity atoms (H, OH, Cl, and F), respectively.

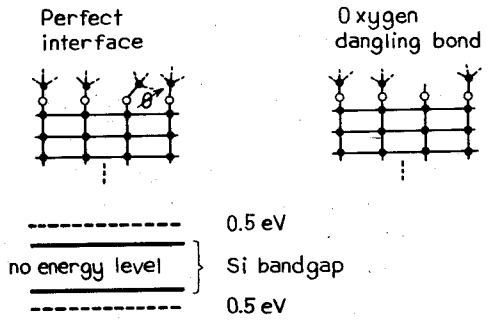

FIG. 9. Perfect interface and oxygen dangling bond at the Si-SiO_2 interface have no energy level in the range between 0.5 eV below the top of the valence band and 0.5 eV above the bottom of the conduction band of Si. Open and closed circles denote O and Si atoms, respectively.

V. RESULTS AND DISCUSSIONS

Both the perfect interface with the Si-O-Si bond angle ranged from 120° to 180° and the interface with oxygen dangling bond do not have a gap state as illustrated in Fig. 9. However, $Si_3{\equiv}Si$- dangling bond at the interface gives rise to a gap state at about the middle of the Si band gap as shown in Fig. 10, as Laughlin *et al.*[2] have indicated. But it should be noted that the Si band gap in their calculation was about 2.5 eV owing to the nearest-neighbor approximation and a Bethe-lattice approximation for the Si substrate, whereas in our model the Si band gap is calculated to be exactly 1.1 eV.

The O-vacancy and Si-Si weak bond at the interface

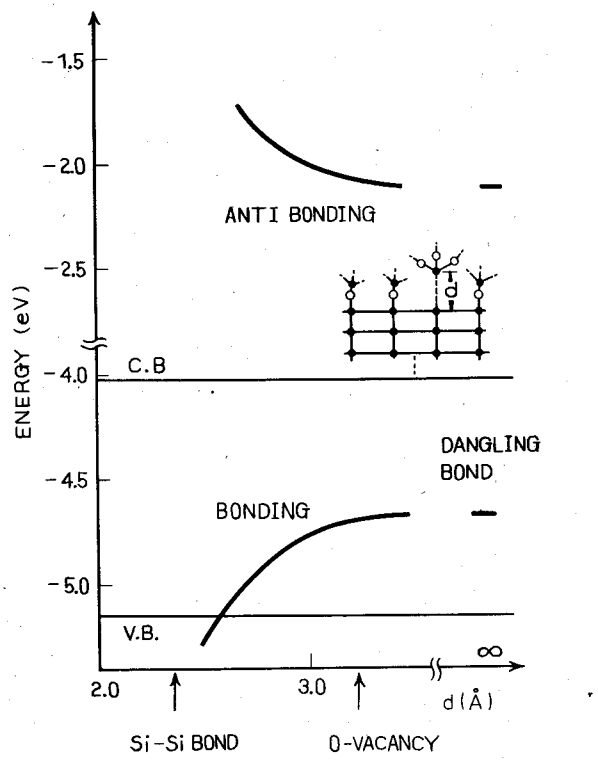

FIG. 10. Si dangling bond, Si-Si bond, and O-vacancy level at the interface. These energy levels move in the lower half of the Si band gap with changing the bond length d. Open and closed circles denote O and Si atoms, respectively.

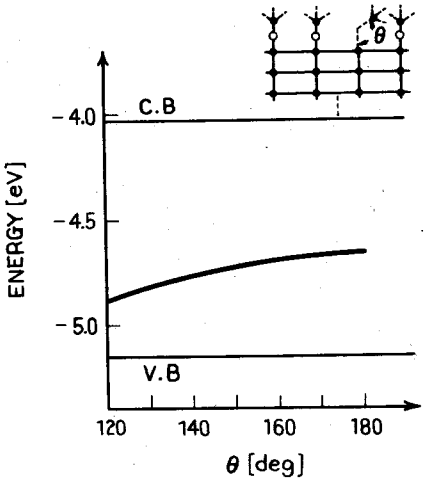

FIG. 11. O-vacancy level and its dependence on the bond bending angle. Open and closed circles denote O and Si atoms, respectively.

produce trap states in the Si band gap, whose energy levels vary in the energy range lower than the midgap of Si by changing various bonding parameters. Figure 10 demonstrates the dependence of the Si-Si weak bond level (including the O-vacancy level) on the Si-Si bond length. Figures 11 and 12 show how the O-vacancy level varies in energy depending on the bond bending angle, and the rotation angle, respectively. In these bonding parameters, bond length variation gives the strongest effect on the energy level.

When the Si dangling bond interacts weakly with the Si atom which is already bonded to four oxygen atoms in the SiO_2 network, the level also appears in the Si band gap. This level moves in the lower half of the Si band gap when the distance between these two Si atoms are varied from 2.3 Å to infinity as is shown in Fig. 13.

On the contrary, Si-O weak bonds and Si-O weak interaction produce trap levels in the upper half of the Si band

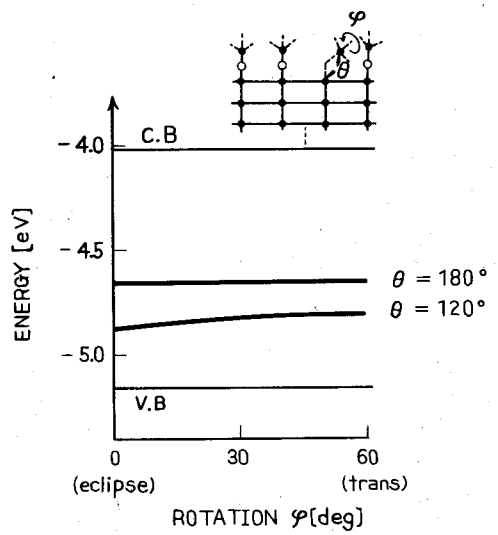

FIG. 12. Dependence of O-vacancy level on the bond rotation angle. This dependence is very weak. Open and closed circles denote O and Si atoms, respectively.

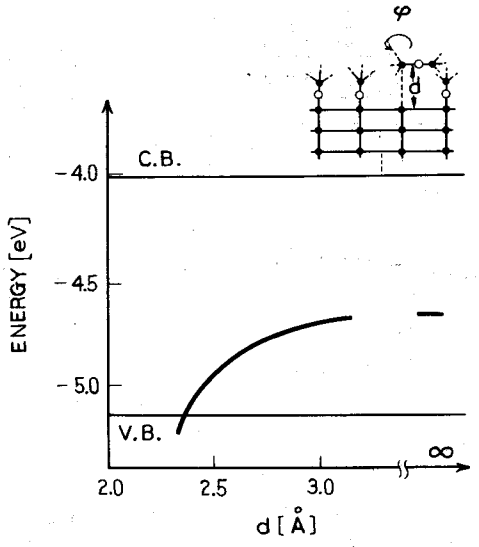

FIG. 13. Energy level of Si dangling bond weakly interacting with Si atom which is already bonded to four oxygen atoms in SiO_2 network. The energy level varies with changing the distance d. φ rotation gives no significant effect on the energy level. Open and closed circles denote O and Si atoms, respectively.

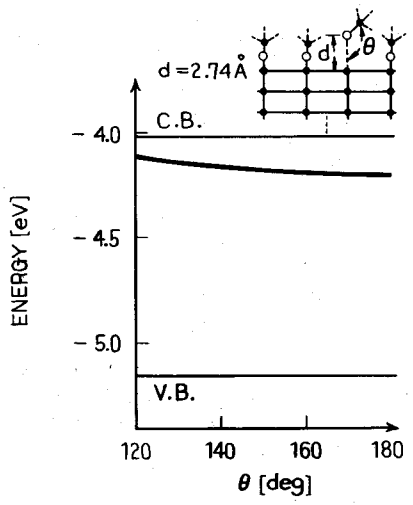

FIG. 15. The dependence of the energy level of Si-O weak bond on bond bending angle. The dependence is minor. Open and closed circles denote O and Si atoms, respectively.

gap. The Si-O weak bond state changes its energy level depending on the bond length and the bond bending angle as demonstrated in Figs. 14 and 15, respectively. Si-O weak interaction indicates situation where the Si dangling bond interacts weakly with the O atom which is already bonded to two Si atoms in the SiO_2 network. Figure 16 shows the dependence of the Si-O weak interaction level on the distance between the Si atom and the O atom.[21] The various energy levels mentioned above are summarized in Fig. 17.

The bonding parameters at the actual Si-SiO_2 interface can be supposed to vary because of the amorphous structure and the large internal stress included in this system. Therefore Si-Si weak bond, Si-Si weak interaction, Si-O weak bond, and Si-O weak interaction are thought to be the possible origins of the interface trap states continuously distributed in energy. Commonly observed U-shaped distribution of the interface trap densities (Fig. 18) is explained, if bond length distributions in Fig. 19 and energy level dependences on the bond length as Fig. 10 and Fig. 14 are assumed. The rapid decrease of the distribution (Fig. 19) as the bond length increases is reasonable because the normal bond lengths are shorter than 2.5 Å and the longer bond lengths are less likely.

The gap states move out of the energy range between 0.5 eV below the top of Si valence band and 0.5 eV above the bottom of Si conduction band when any of H, OH, Cl, or F is bonded to the Si atom at the interface. This situation is illus-

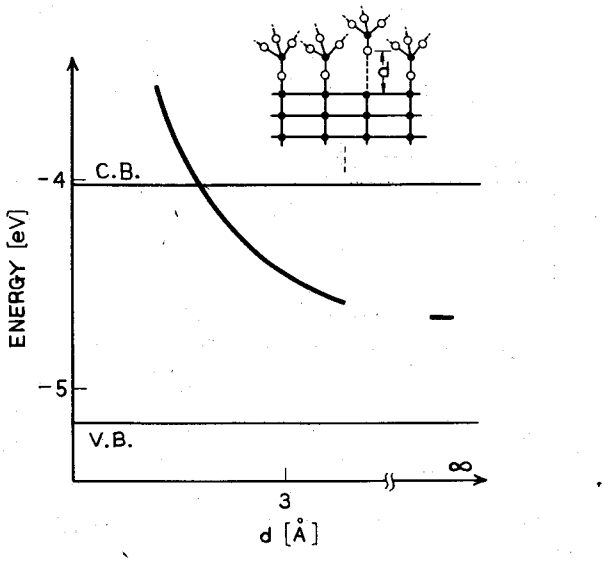

FIG. 14. Energy level of Si-O weak bond at the interface. This energy level moves in the energy range higher than the midgap with changing the bond length d. Open and closed circles denote O and Si atoms, respectively.

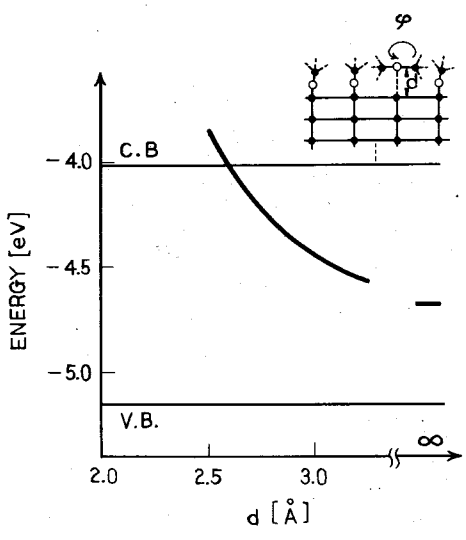

FIG. 16. Energy level of Si dangling bond weakly interacting with oxygen atom which is already bonded to two Si atoms in SiO_2 network. The energy level varies with changing the distance d. φ rotation gives no significant effect on the energy level. Open and closed "cirlces" denote O and Si atoms, respectively.

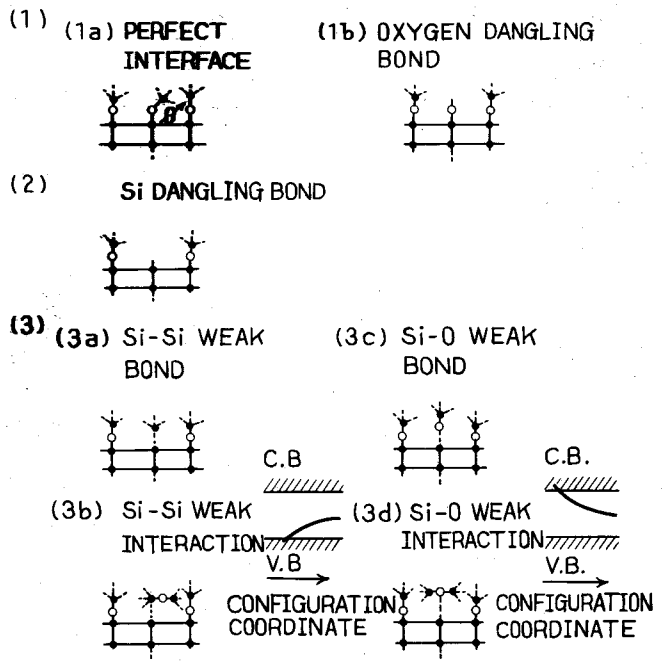

FIG. 17. Summary of various energy levels at the Si-SiO_2 interface. (1) Perfect interface (1a) and the interface containing oxygen dangling bond (1b) have no energy level in the Si band gap. (2) $Si_3{\equiv}Si$- dangling bond has an energy level at about the midgap of Si. (3) Si-Si weak bond (3a) Si-Si weak interaction (3b), Si-O weak bond (3c), and Si-O weak interaction (3d), give rise to gap states whose energy levels vary within the forbidden gap of Si with the change of the configurations. Open and closed circles denote O and Si atoms, respectively.

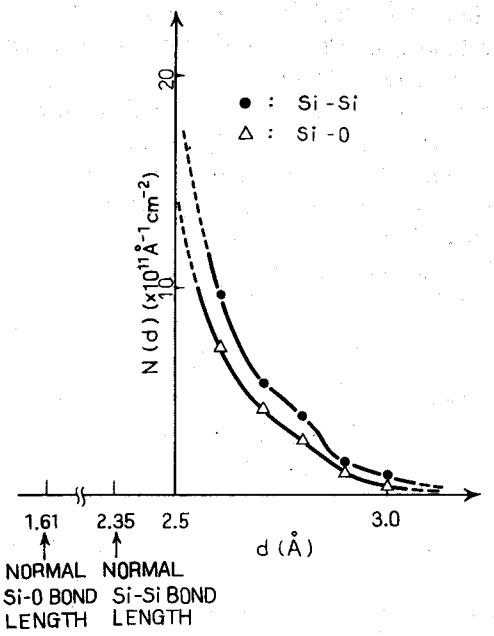

FIG. 19. Assumed bond length density $N(d)$ ($Å^{-1}$ cm^{-2}) vs bond length d (Å). Using this distribution together with the energy level dependence on bond length of Fig. 10 and Fig. 14, U-shaped distribution as shown in Fig. 18 can be explained.

trated in Fig. 20. Since an energy level outside the Si band gap can not work as a trap state at the interface under normal operating conditions, this result explains the reduction of the interface trap density by H_2 annealing, trichrolo-ethylene annealing, and HCl oxidation, and further suggests the possibility of F annealing.

VI. CONCLUSIONS

A calculation procedure dealing with the electronic structures of crystalline Si-amorphous SiO_2 interface including microstructural defects is presented based on semiempirical tight-binding Hamiltonians and Green's function formulation and applied to the calculation of interface trap states between amorphous SiO_2 and the Si substrate with (111) orientation.

The following results are obtained. The perfect interface and the interface including oxygen dangling bonds have no energy level in the Si band gap, whereas the $Si_3{\equiv}Si$- dangling bond has an energy level at about the middle of the Si band gap. Si-Si weak bond and weak interaction at the interface give rise to gap states whose energy move in the energy range lower than the midgap with varying the distances between two Si atoms, while the energy levels of Si-O weak

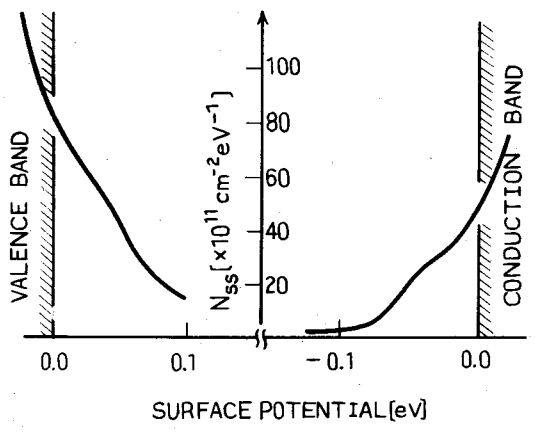

FIG. 18. Commonly observed U-shaped distribution of interface trap-state density in the forbidden gap of Si. (cited from Ref. 22).

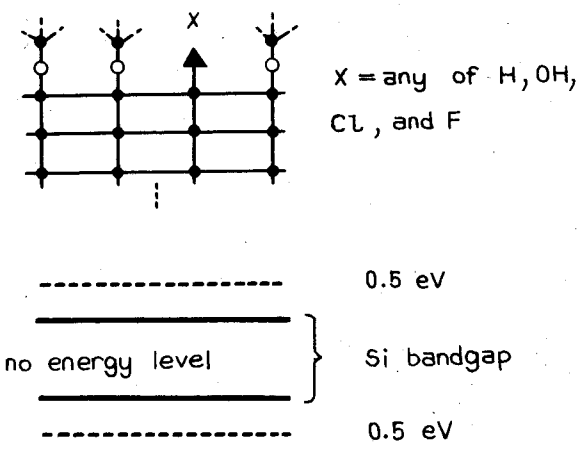

FIG. 20. Impurity at the Si-SiO_2 interface. If any of H, OH, Cl, and F is bonded to the Si dangling bond, no energy level exists in the energy range between 0.5 eV below the top of the valence band and 0.5 eV above the bottom of the conduction band of Si. Open and closed circles denote O and Si atoms, respectively.

bond and weak interaction at the interface appear at the upper half of the forbidden gap of Si depending on the distances between the Si atom and the O atom.

Possible origins of interface trap states which are distributed continuously in the Si energy gap are suggested to be these Si-Si weak bonds, Si-Si weak interactions, Si-O weak bonds, and Si-O weak interactions, at the interface.

The reduction of the gap state density by H_2 annealing, trichrolo-ethylene annealing, or HCl oxidation is understood by bonding H or Cl to the $Si_3{\equiv}Si$- dangling bond at the interface.

ACKNOWLEDGMENT

We express our sincere thanks to Doctor Y. Okabe at the University of Tokyo for helpful discussions in the course of this study.

APPENDIX A

Calculation of $(EI - H)G = I$ using

$$\begin{pmatrix} G_{AA} & G_{AB} \\ G_{BA} & G_{BB} \end{pmatrix} = \begin{pmatrix} g_{AA}^{-1} & -V_{AB} \\ -V_{BA} & g_{BB}^{-1} \end{pmatrix} \tag{A1}$$

leads to

$$\begin{pmatrix} G_{AA}^{22} & G_{AA}^{21} \\ G_{AA}^{12} & G_{AA}^{11} \end{pmatrix}$$

$$= \begin{pmatrix} g_{AA}^{22} + g_{AA}^{21} V_{AB}^{11} G_{BA}^{12} & g_{AA}^{21} + g_{AA}^{21} V_{AB}^{11} G_{BA}^{11} \\ g_{AA}^{12} + g_{AA}^{11} V_{AB}^{11} G_{BA}^{12} & g_{AA}^{11} + g_{AA}^{11} V_{AB}^{11} G_{BA}^{11} \end{pmatrix} \tag{A2}$$

and

$$\begin{pmatrix} G_{BA}^{12} & G_{BA}^{11} \\ G_{BA}^{22} & G_{BA}^{21} \end{pmatrix} = \begin{pmatrix} g_{BB}^{11} V_{BA}^{11} G_{AA}^{12} & g_{BB}^{11} V_{BA}^{11} G_{AA}^{11} \\ g_{BB}^{21} V_{BA}^{11} G_{AA}^{12} & g_{BB}^{21} V_{BA}^{11} G_{AA}^{11} \end{pmatrix}. \tag{A3}$$

Particularly, the following equations are useful:

$$G_{AA}^{11} = g_{AA}^{11} + g_{AA}^{11} V_{AB}^{11} G_{BA}^{11}, \tag{A4}$$

$$G_{BA}^{11} = g_{BB}^{11} V_{BA}^{11} G_{AA}^{11}. \tag{A5}$$

Substituting Eq. (A5) into Eq. (A4) and solving for G_{AA}^{11}, we have Eq. (9). Other than Eq (9) and Eq. (10),

$$G_{AA}^{11} = g_{AA}^{11} V_{AB}^{11} G_{BB}^{11} V_{BA}^{11} g_{AA}^{11} + g_{AA}^{11} \tag{A6}$$

also holds.

[1] D. J. Chadi, R. B. Laughlin, and J. D. Joannopoulos, *The Physics of SiO_2 and Its Interfaces* (Pergamon, New York, 1978), p. 55.
[2] R. B. Laughlin, J. D. Joannopoulos, and D. J. Chadi, in Ref. 1, p. 321.
[3] R. B. Laughlin, J. D. Joannopoulos, and D. J. Chadi, Phys. Rev. B **21**, 5733 (1980).
[4] J. D. Joannopoulos and F. Yndurain, Phys. Rev. B **10**, 5164 (1974).
[5] F. J. Grunthaner and J. Maserjian, Phys. Rev. B **10**, 389 (1978).
[6] C. R. Helms, Y. E. Strausser, and W. E. Spicer, Appl. Phys. Lett. **33**, 767 (1978).
[7] W. T. Pantelides and M. Long, *The Physics of SiO_2 and Its Interface* (Pergamon, New York, 1978), p. 339.
[8] A. Koma (private communication).
[9] R. L. Mozzi and B. E. Warren, J. Appl. Crystallogr. **2**, 164 (1969).
[10] H. R. Philipp, Solid State Commun. **4**, 73 (1966).
[11] K. C. Pandey and J. C. Phillips, Phys. Rev. B **13**, 750 (1976).
[12] G. Dresselhaus and M. S. Dresselhaus, Phys. Rev. **160**, 649 (1967).
[13] D. J. Chadi, Phys. Rev. B **16**, 790 (1977).
[14] K. C. Pandey and J. C. Phillips, Solid State Commun. **14**, 459 (1974).
[15] J. Pollmann and S. T. Pantelides, Phys. Rev. B **18**, 5524 (1978).
[16] N. P. Il'in and V. F. Masterov, Soviet Phys. Semicond. **11**, 874 (1977).
[17] H. Basch, A Viste, and H. B. Gray, Theor. Chim. Acta **3**, 458 (1965).
[18] T. Shimizu and N. Ishii, Report of Eng. Dept. of Kanazawa Univ. **11**, 11 (1977).
[19] E. Clementi and D. L. Raimondi, J. Chem. Phys. **38**, 2686 (1963).
[20] R. B. Laughlin and J. D. Joannopoulos, Phys. Rev. B **17**, 2790 (1978).
[21] In calculating the energy levels of Si-Si weak interactions shown in Fig. 13 and those of Si-O weak interactions shown in Fig. 16, the interaction parameters among atoms having normal valency have been used. To weaken these interaction parameters is almost equivalent to increase the distance between the atoms at the interface.
[22] H. Sakaki, K. Hoh, and T. Sugano, IEEE Trans. Electron. Devices **ED-17**, 892 (1970).